Springer

Journal of Mechanical Science and Technology 23 (2009) 2928~2937

Journal of Mechanical Science and Technology

www.springerlink.com/content/1738-494x
DOI 10.1007/s12206-009-0808-3

Automated design system for a rotor with an ellipse lobe profile †

Sung-Yuen Jung[1], Seung-Moo Han[2], Hae-Yong Cho[3] and Chul Kim[1,*]

[1]*Research Institute of Mechanical Technology, Pusan National University, JangJeon-Dong, Keumjung-Ku, Busan 609-735, Korea*
[2]*Department of Biomedical Engineering, Kyung Hee University, Seoul 130-731, Korea*
[3]*Department of Mechanical Engineering, Chungbuk National University, Cheongju-si Chungbuk 361-763, Korea*

(Manuscript Received April 3, 2009; Revised July 8, 2009; Accepted July 14, 2009)

Abstract

An internal lobe pump (ILP) is suitable for machine tool oil hydraulics, automotive engines, compressors, and various other devices. In particular, the ILP is an essential component of an automotive engine, used to feed lubricant oil through the system. The main components of an ILP are its rotors. The outer rotor is typically characterized by lobes with an elliptical shape, and the inner rotor profile is a conjugate to the outer profile. This paper describes a theoretical analysis of an ILP and the development of an integrated automated system for rotor design. This system is composed of three main modules and has been developed using AutoLISP for the AutoCAD program. The system generates a new lobe profile and automatically calculates flow rate and flow rate irregularity according to the lobe profile generated. Results obtained from the analysis can enable oil pump designers and manufacturers to become more efficient.

***Keywords*:** Elliptical lobe; Flow rate irregularity; Internal lobe pumps; Specific flow rate; Specific slipping

1. Introduction

Internal gear pumps are widely used as lubricant suppliers and as hydraulic source of engine lubrication for automatic transmissions due to the low level of noise generated by their inner and outer rotors compared with to other types of pumps. Colbourne [1] obtained the coordinates of the inner rotor lobes by simulating the contact between the inner and outer rotors, and calculating the area of the chamber closed by the lobe curve of the same. Sae-gusa et al. [2] obtained the trajectory measurements of the arc centers and lobes of the outer rotor by fixing the inner rotor and rotating the outer rotors, after which they and derived a formula to obtain the lobes of the inner rotor from the engagement characteristics of the inner and outer ones. Recently, Tsay [3, 4] described the process of obtaining the lobes of the inner rotor by simulating the cutting process. Lee et al. [5] performed an analysis of the operational characteristics, while Kim et al. [6] observed the change in contact stress pursuant to gerotor design variables. In addition, Kim et al. [7-9] suggested a new method to derive lobe equations for the trochoid lobe of the gerotor pumps when the lobe profile of the outer rotor is a circle. In addition, they established an integrated system to automatically obtain the trajectories of the inner and outer rotors and contact points, the rotation simulation, the flow rate and flow rate irregularity, and other parameters.

This research establishes an automated rotor design system using a kinetic analysis that considers design variables from the outer rotor with an ellipse lobe profile. First, we entered the number of outer rotor lobes z_2, the distance between the inner and outer rotor centers (also known as eccentricity) e, the minor axis distance of ellipse r_{12}, the distance between the outer rotor center point and the ellipse center d, the major-minor axis ratio of ellipse k, and the design variable values of tip gap t_p into the design automation system. The system then creates inner and outer rotors within a

† This paper was recommended for publication in revised form by Associate Editor Jooho Choi

*Corresponding author. Tel.: +82 51 510 2489, Fax.: +82 51 512 9835
E-mail address: chulki@pusan.ac.kr

generation field range with no cusps and loops (these are geometric design limits), and automatically calculates flow rate, flow rate irregularity, and slipping for the created rotor. This system then displays these results in graphical form.

2. Mechanism and kinematics of the rotor

Lobe equations were derived by rotating outer rotors around the center O_2 of the pitch circle with pitch point P (r_2,0), where the pitch circles of the inner and outer rotors intersect and are fixed. Fig. 1 shows the center O_2 of the outer rotor pitch circle; the center O_1 of the inner rotor pitch circle; the eccentricity e, the distance between O_2 and O_1 and the intersection point C'(x',0) between the normal line at the initial start point A(x_0,y_0) and x-axis and the line segment from the center point of the outer rotor pitch circle to the ellipse center when the outer rotor is a part of a curvature with an ellipse profile.

The number of outer rotor lobes and the pitch circle radius of the inner and outer rotors are described as follows:

$$z_2 = z_1 + 1\,,\quad r_1 = ez_1\,,\quad r_2 = ez_2 \tag{1}$$

The distance ρ from the ellipse center to the initial start point A(x_0,y_0) is obtained using Eqs. (2) and (3), as shown in Fig. 2:

$$\overline{FB} = \overline{BC}\tan\theta\,,\quad \overline{AB} = \overline{BC}\tan\delta\,,\quad \overline{AB} = k\overline{FB}\,,$$
$$\tan\delta = k\tan\theta \tag{2}$$

$$\rho = r_{l2}\sqrt{\cos^2\theta + k^2\sin^2\theta} \tag{3}$$

To obtain the trajectory of the inner rotor, the outer rotor is rotated counterclockwise as α around the center O_2 of the pitch circle. The angle δ from the ellipse center to the contact point is obtained using Eqs. (4) and (5), as shown in Fig. 3:

$$C'' = \begin{pmatrix} x_1 \\ y_1 \end{pmatrix} = \begin{pmatrix} \cos\alpha & -\sin\alpha \\ \sin\alpha & \cos\alpha \end{pmatrix}\begin{pmatrix} x' \\ 0 \end{pmatrix} \tag{4}$$

$$\xi = \cos^{-1}\left(\frac{\overrightarrow{C''P}\cdot\overrightarrow{C''O_2}}{\left|\overrightarrow{C''P}\right|\left|\overrightarrow{C''O_2}\right|}\right) \tag{5}$$

where $\delta = \arctan(k^2\tan\xi)$.

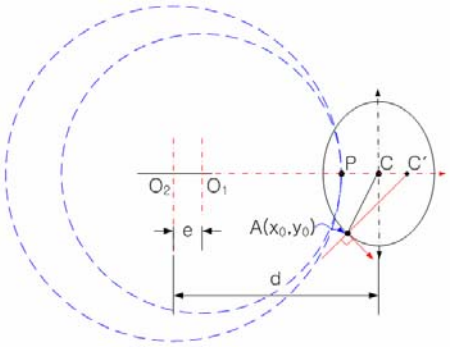

Fig. 1. Conjugated profile tracing.

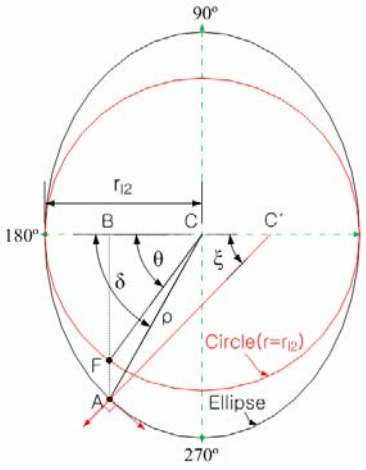

Fig. 2. Conjugated profile tracing for an ellipse.

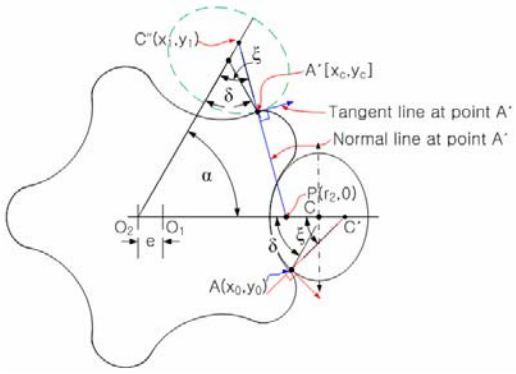

Fig. 3. Center of curvature in the rotated position.

The intersection point between the straight connection line from pitch point P to point C" and the curvature trajectory of the outer rotor is contact point A'. The contact point A' can then be obtained from Eq. (6) for a straight line $\overline{C''P}$ for an ellipse rotated counterclockwise as α. We now have

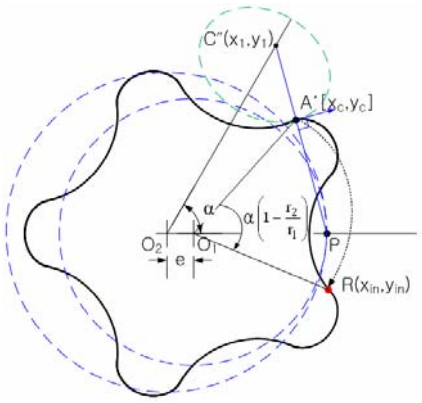

Fig. 4. Inner rotor profile tracing.

$$A' = \begin{pmatrix} x_c \\ y_c \end{pmatrix} = \begin{pmatrix} \cos\alpha & -\sin\alpha \\ \sin\alpha & \cos\alpha \end{pmatrix} \begin{pmatrix} x_0 \\ y_0 \end{pmatrix} \tag{6}$$

where $A = \begin{pmatrix} x_0 \\ y_0 \end{pmatrix} = \begin{pmatrix} d - \rho\cos\delta \\ \rho\sin\delta \end{pmatrix}$.

In Fig. 4, the point R existing on the trajectory of the inner rotor from the contact point A' can be obtained from the following relations:

$$\begin{pmatrix} x_{in} \\ y_{in} \end{pmatrix} = \begin{pmatrix} \cos\alpha' & -\sin\alpha' \\ \sin\alpha' & \cos\alpha' \end{pmatrix} \begin{pmatrix} x_c - e \\ y_c \end{pmatrix} + \begin{pmatrix} e \\ 0 \end{pmatrix} \tag{7}$$

Here, α' can be obtained from the relation in Eq. (8) as follows:

$$\alpha' = \alpha\left(1 - \frac{r_2}{r_1}\right) \tag{8}$$

In Fig. 4, the point existing on the trajectory of the outer rotor from the contact point A' can be obtained from Eq. (9):

$$\begin{pmatrix} x_{out} \\ y_{out} \end{pmatrix} = \begin{pmatrix} \cos\alpha & \sin\alpha \\ -\sin\alpha & \cos\alpha \end{pmatrix} \begin{pmatrix} x_c \\ y_c \end{pmatrix} \tag{9}$$

3. Calculation of the flow rate and flow rate irregularity

The instantaneous flow rate and its irregularity can be calculated using information from the contact points and the inner and outer rotor lobes. Working fluids were assumed to be incompressible, thereby causing no volume change. In Fig. 5, the hatched

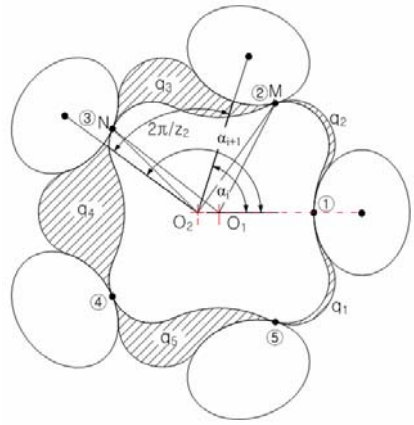

Fig. 5. Evaluation of the contribution to the flow rate given by each flank of rotors.

chamber is a closed area around the boundary of two contact points where the inner and outer rotors meet. Minute angular rotations of the rotor changes the side length of each chamber to increase or decrease its volume. In this case, the areas shown by the fields where suction and discharge occur are proportional to the square of the distance between the center and the contact point. Thus, the instantaneous flow rate indicating the level that the chamber contributes to the change of flow rate can be obtained from:

$$q_i(\alpha) = \frac{1}{2} b \left[\left(\left|\overrightarrow{O_1M}\right|^2 - \left|\overrightarrow{O_1N}\right|^2 \right) \frac{r_2}{r_1} - \left(\left|\overrightarrow{O_2M}\right|^2 - \left|\overrightarrow{O_2N}\right|^2 \right) w_1 \right] \tag{10}$$

In Fig. 5, the distance from the center point of the inner and outer rotors to the starting contact point (M) and end contact point (N) of the i^{th} chamber can be obtained from Eqs. (11) and (12), respectively:

$$\left|\overrightarrow{O_1M}\right| = \rho_{i,1}, \quad \left|\overrightarrow{O_2M}\right| = \rho_{i,2} \quad (\alpha = \alpha_i) \tag{11}$$

$$\left|\overrightarrow{O_1N}\right| = \rho_{i+1,1}, \quad \left|\overrightarrow{O_2N}\right| = \rho_{i+1,2} \quad (\alpha = \alpha_{i+1}) \tag{12}$$

Here, $\alpha_{i+1} = \alpha_i + \frac{2\pi}{z_2}$.

Eq. (13) describes the flow rate per revolution:

$$Q = z_1 \int_0^{2\pi} q(\alpha) d\alpha = z_1 \sum_{i=1}^{z_2} q_i \tag{13}$$

The specific flow rate is obtained from Eq. (14):

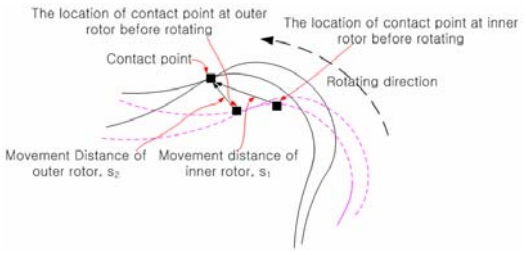

Fig. 6. Evaluation of the contribution to specific slipping.

$$R = \frac{Q}{\pi \rho_{i,\max}^2 b} \tag{14}$$

The flow rate irregularity affecting noise and vibration is described by Eq. (15):

$$i = \frac{q_{\max} - q_{\min}}{q_{average}} \tag{15}$$

Specific slipping can be obtained from Eq. (16):

$$S.S. = \frac{|s_2 - s_1|}{s_2} \tag{16}$$

Here, s_1 and s_2 refer to the movement distances of contact points from the inner and outer rotor profiles, respectively, according to the number of revolutions, as shown in Fig. 6.

4. Automatic system

4.1. System configuration

An integrated design automation system was developed using the AutoLISP for the AutoCAD program to create an outer rotor with an elliptical lobe profile. Our system consists of input, design, and output modules. A schematic diagram of the system is shown in Fig. 7.

4.1.1 Input module

The input module facilitates the inputting of design variable values in order to automate the design of the lobe and perform calculations for flow rate, flow rate irregularity, and slipping. Input variables include the number of outer rotor gears z_2, the distance between inner and outer rotor centers (eccentricity) e, the minor axis distance of the ellipse r_{l2}, the distance between the outer rotor center O_2 and the ellipse center C, the major/minor axis ratio of ellipse k , and the tip gap tp. Fig. 8 shows the graphical input window of the design automation system.

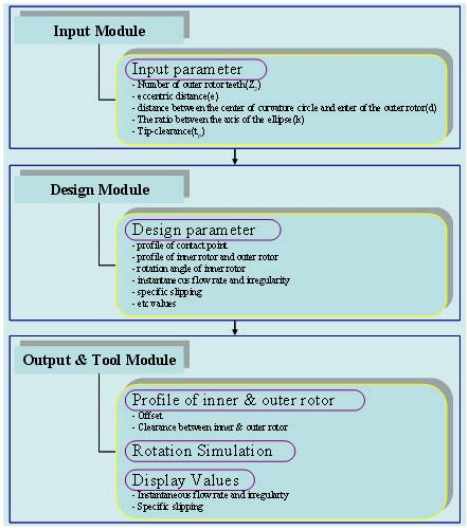

Fig. 7. Configuration of the system.

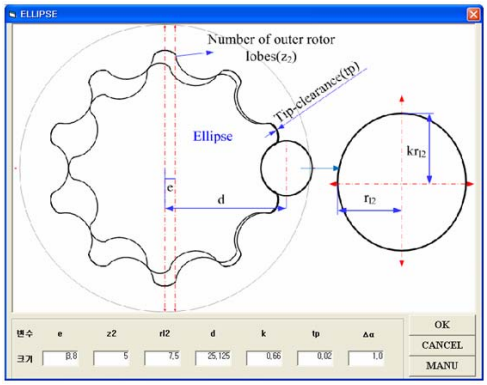

Fig. 8. The input window of the system.

4.1.2 Design module

The design module calculates the trajectory of the inner rotor from the outer rotor using a lobe profile equation from the inputted design variable values. It also compensates for the offset quantity between the inner and outer rotors, and then calculates the flow rate, its irregularity, and the slipping of the created lobe profile. The algorithm to create the trajectory of the inner rotor is shown in Fig. 9(a), and the algorithm to calculate the instantaneous flow rate and its irregularity is shown in Fig. 9(b). The inner rotor profile, the flow rate, and the specific slipping for the case of k=1.3 are automatically generated by the system, as shown in Fig. 10.

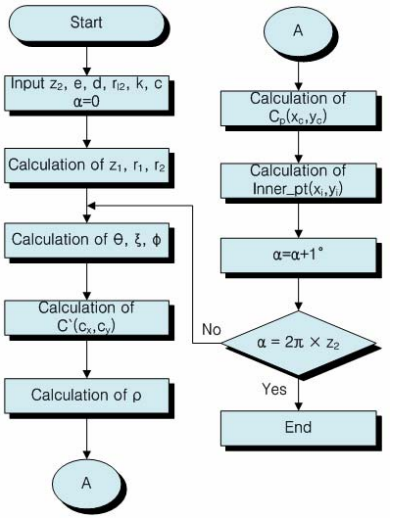

(a) The lobe profile

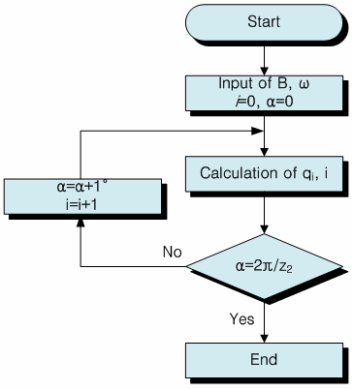

(b) Flow rate and irregularity

Fig. 9. Flowchart for operating the automated system.

4.1.3 Output module

The output module performs lobe modeling, rotation simulation, as well as storage of instantaneous flow rate curves and data files. The output module contains two sub-modules. The sub-module for the lobe profile modeling of the output module receives the curvature of the outer rotor end, the distance between inner and outer rotors, the offset quantity of the inner rotor, and the rotation angle of the inner rotor. It then creates a lobe profile according to the rotation angle, using the trajectories of the inner and outer rotors obtained from the design module. Meanwhile, the sub-module for rotation simulation prevents users from making errors by checking the chamber profile and size and the rotation interference, among others, by simulating the rotation shape of the actual inner and outer rotors, as shown in Fig. 11.

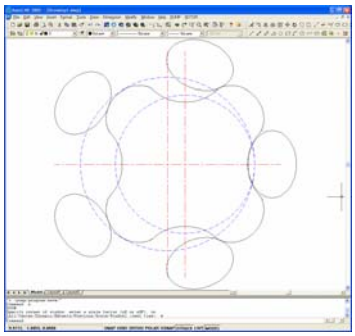

(a) The inner rotor profile

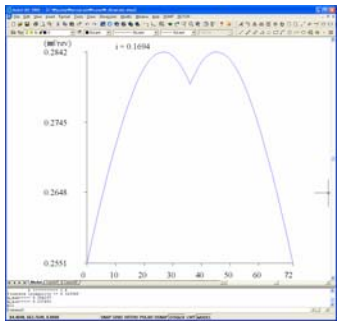

(b) The flow rate

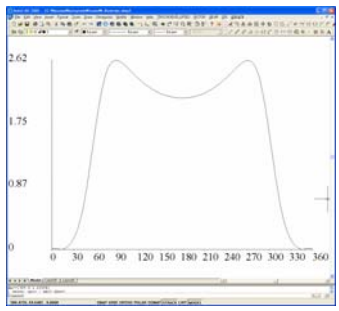

(c) The specific slipping

Fig. 10. The inner rotor profile, the flow rate and the specific slipping generated by the system.

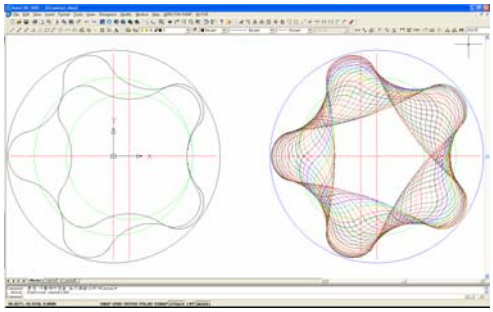

Fig. 11. The results carried out at the rotation simulation submodule of the design module.

4.2 Application to the system and its review

For functionality within a range causing no cusp or loop within a permitted pressure angle, the flow rate and its irregularity were first considered. Afterwards, showing a tendency to affect the lifespan, slipping was calculated next. The inner and outer rotors have 4/5 teeth with parameters as follows: outer rotor eccentricity e=3.8 mm, width w=18.0 mm, and outer diameter φ=58 mm. The inner rotor relative to the outer rotor with an elliptical profile was created with the design variable values shown in Table 1 by changing the curvature radius r_{12} of the ellipse, the distance d up to the curvature radius, and the major/minor axis ratio k of the ellipse (which are the optimum design variables) to maintain the distance between the maximum outer diameter and the lobe bottom diameter of the outer rotor at a constant value of 3.75 mm (see Fig. 12).

Fig. 13 shows the lobe profile created by simulation while changing the center distance d, the curvature radius r_{12}, and the major/minor axis ratio k. The values of the flow rate and its irregularity that have been calculated automatically for the created lobe profile are shown in Table 1. The maximum flow rate was obtained when the values of r_{12} were at 11.0 and 12.0. The major/minor axis ratio k was 0.9 from Fig. 14(a). This value shows that a maximum flow rate was obtained as the center distance d and curvature radius r_{12} increased, and as the major/minor axis ratio k decreased. Fig. 14(b) shows that the flow rate irregularity also decreased as the major/minor axis ratio decreased.

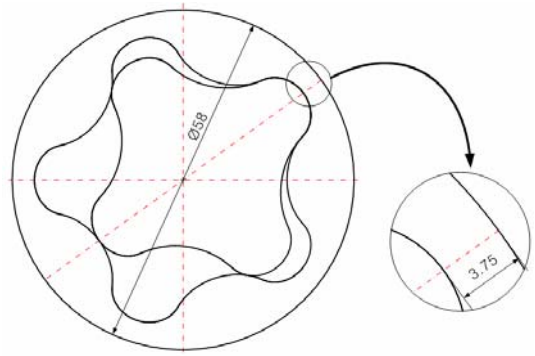

Fig. 12. The distance between the outer diameter and the base circle of the outer rotor.

Table 1. The values of the input variable parameters.

d	r_{12}	K	i (%)	Q(cc/rev)
25.125	7.5	0.6	7.5648	0.9998
		0.7	8.1412	1.001
		0.8	8.6746	1.002
		0.9	9.189	1.0028
		1.1	10.178	1.0036
		1.2	10.655	1.0037
		1.3	11.1125	1.0035
25.625	8	0.6	7.67	1.0002
		0.7	8.2692	1.0014
		0.8	8.8214	1.0024
		0.9	9.3524	1.0031
		1.1	10.3663	1.0037
		1.2	10.8489	1.0037
		1.3	11.3176	1.0034
26.625	9	0.6	7.8715	1.001
		0.7	8.5141	1.002
		0.8	9.0986	1.0029
		0.9	9.6556	1.0035
		1.1	10.715	1.0038
		1.2	11.2154	1.0036
		1.3	11.1125	1.0035
27.625	10	0.6	8.0619	1.0016
		0.7	8.743	1.0026
		0.8	9.3576	1.0034
		0.9	9.94	1.0038
		1.1	11.0327	1.0038
		1.2	11.5412	1.0034
		1.3	12.0306	1.0029
28.625	11	0.6	8.237	1.0022
		0.7	8.9542	1.0031
		0.8	9.5962	1.0037
		0.9	10.1986	1.004
		1.1	11.3248	1.0037
		1.2	11.8456	1.0032
		1.3	12.3334	1.0026
29.625	12	0.6	8.4069	1.0027
		0.7	9.1595	1.0034
		0.8	9.8253	1.0039
		0.9	10.447	1.004
		1.1	11.5916	1.0035
		1.2	12.1213	1.0029
		1.3	12.6183	1.0022

k \ d,r_{l2}	25.125, 7.5	25.625, 8.0	26.625, 9.0	27.625, 10.0	28.625, 11.0	29.625, 12.0
0.6	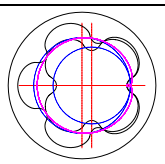	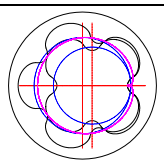	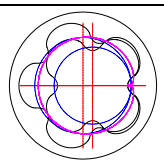	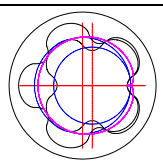	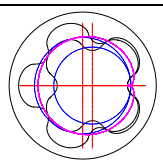	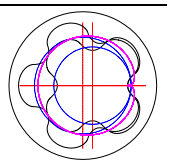
0.7	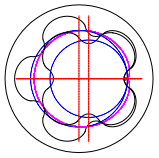	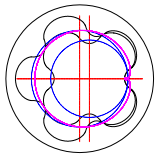	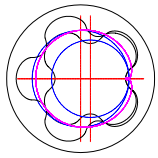	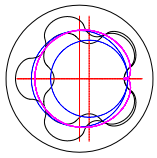	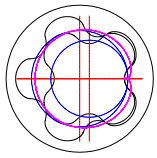	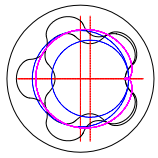
0.8	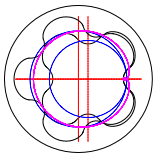	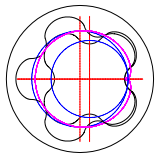	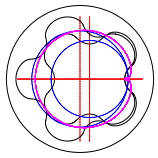	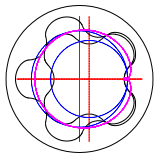	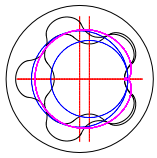	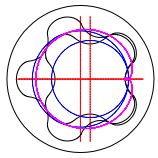
0.9	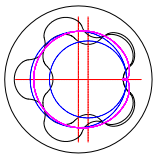	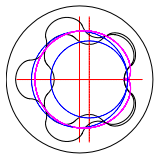	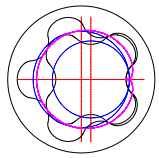	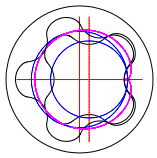	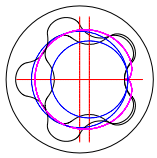	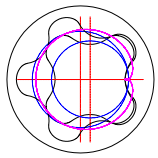
1.0	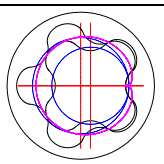	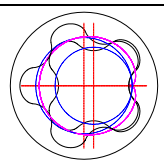	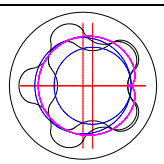	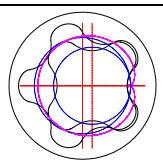	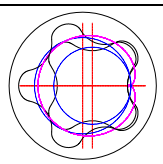	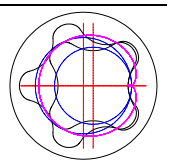
1.1	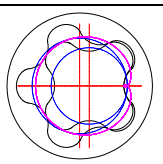	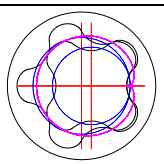	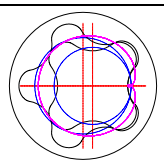	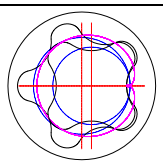	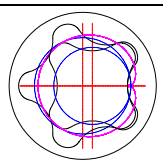	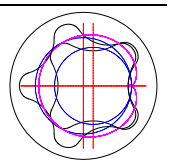
1.2	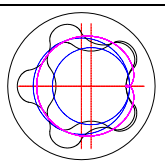	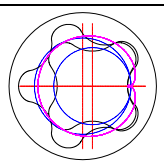	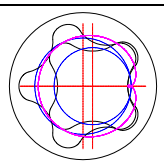	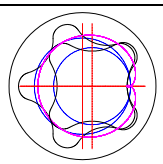		
1.3						

Fig. 13. Results carried out in the system according to the variable parameters.

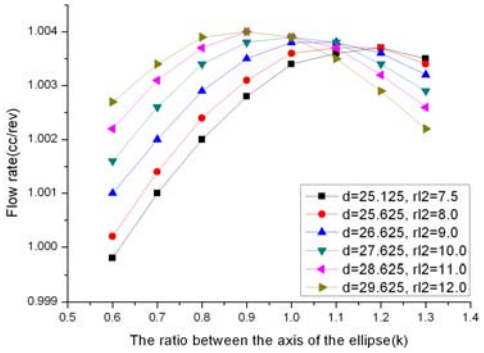

(a)

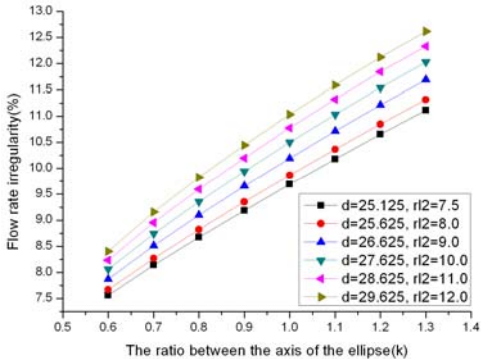

(b)

Fig. 14. A comparison of irregularity and flow rate according to the factor, k: (a) flow rate, (b) flow rate irregularity.

4.3 Production and review prototype

Figs. 15(a) and (b) are the rotors for internal gear pumps currently used in diesel-run passenger cars. They have the following characteristics: 4/5 teeth; outer diameter of outer rotor φ=58 mm; eccentricity e=3.8 mm; number of teeth z_2=5; and width w=18.0 mm. The values of the design factors obtained from the system while changing the major/minor axis ratio k of the ellipse in order to develop a rotor with better performance are k=0.66 and 1.3; r_{12}=7.5 and 8; and d=25.125 and 25,625. The actual flow rates of the rotors shown in Figs. 15(c) and (d), along with the preceding design factor values were compared with the values of the rotors currently used in diesel-run passenger cars.

The developed rotor products (see Figs. 15(c) and (d)) with an elliptical lobe profile are better in terms of flow rate or flow rate irregularity. Specifically, the product in Fig. 15(c), which has a low major/minor axis ratio, has the best flow rate irregularity, as shown in Table 2.

Table 2. The results of flow rate and irregularity shown in Fig. 15.

No.	k	r_{12} (mm)	d (mm)	i (%)	Q (cc/rev)
(a)	1.0	14.7	31.4	12.4775	0.9534
(b)	1.0	15.048	32.1	12.2236	0.9724
(c)	0.66	7.5	25.125	7.9165	1.0005
(d)	1.3	8	25.625	11.3176	1.0034

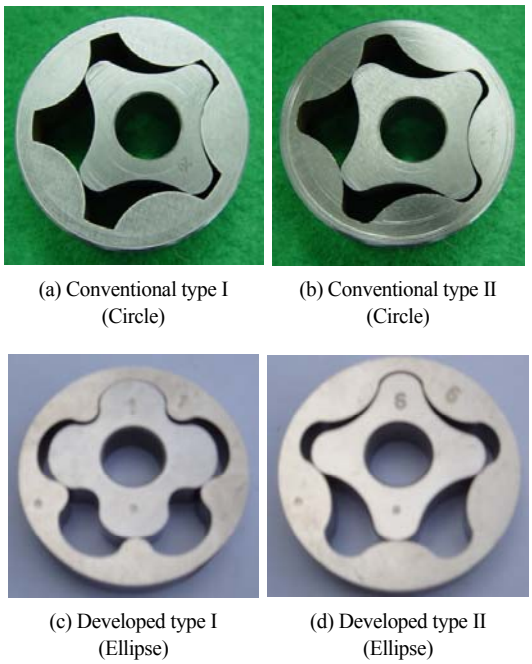

(a) Conventional type I (Circle) (b) Conventional type II (Circle)

(c) Developed type I (Ellipse) (d) Developed type II (Ellipse)

Fig. 15. The products with the input values of Table 2.

5. Conclusions

In this study, we proposed configuration equations for rotors by a geometric analysis of outer rotors with an elliptical lobe profile. Afterwards we created an inner rotor lobe profile based on the result. In addition, we developed an integrated rotor design automation system for oil pumps by computerizing the complicated process that accompanies the calculation of the inner/outer rotor volume, the flow rate, and the flow rate irregularity. We predict that developed automation systems will progress in the future as follows:

(1) Rotors that perform better than the rotors currently used in diesel-run passenger cars can be developed by automatically creating an inner rotor profile, and by developing an integrated design automation system to automatically calculate flow rate and flow rate irregularity for the created rotor profile.

(2) An output module can create a lobe profile via the input variable values, automatically calculate the instantaneous flow rate and its irregularity pursuant to the rotation angle of the outer rotor, and display these results in graphical form.
(3) Design errors can be prevented by simulating the rotation appearance of rotors, which will help manufacturers determine the proper lobe profiles according to specifications given by car makers.

Acknowledgment

This research was financially supported by Pusan National University through the program, Post-Doc. 2008, and the Ministry of Education, Science Technology (MEST) and the Korea Industrial Technology Foundation (KOTEF) through the Human Resource Training Project for Regional Innovation.

Nomenclature

A' : Inner and outer rotor contact point.
b : Rotor thickness.
C : Center point of the curvature radius.
C' : Intersection point between normal line and central axis at the initial contact point of the ellipse.
C" : Rotation point of C' after rotation of outer rotor.
d : Distance between the center of outer rotor and the center of curvature radius.
e : Eccentricity between inner and outer rotors.
i : Flow rate irregularity.
k : Ellipse shape factor.
O_1 : Center point of the inner rotor.
O_1 : Center point of the outer rotor.
P : Locus point of the inner rotor.
R : Specific flow rate.
r_{12} : Curvature radius of the ellipse.
r_1 : Pitch radius of the inner rotor.
r_2 : Pitch radius of the outer rotor.
s_1 : Movement distance of inner rotor.
s_2 : Movement distance of outer rotor.
S.S : Specific slipping.
Q : Flow rate per rotation.
z_1 : Number of the inner rotor lobes.
z_2 : Number of the outer rotor lobes.

Greek

α : Rotational angle of the outer rotor.
α' : Angle between contact point and inner rotor point.
δ : Lobe pressure angle.
θ : Parameter for ellipse equation.
ρ : Distance from the center of the ellipse to the contact point.
φ : Rotational angle of the inner rotor.
ω_1 : Rotor angular velocity.

References

[1] J. R. Colbourne, Gear shape and theoretical flow rate in internal gear pumps, *Transactions of the CSME*, 3 (4) (1975) 215-223.
[2] Y. Saegusa, K. Urashima, M. Sugimoto, M. Onoda and T. Koiso, Development of oil-pump rotors with a trochoidal tooth shape, *SAE Paper*, 93 (3) (1984) 3359-3364.
[3] C. B. Tsay and C. Y. Yu, Mathematical model for the profile of gerotor pumps, *J. CSME*, 10 (1) (1989) 41-47.
[4] C. Y. Yu and C. B. Tsay, The mathematical model of gerotor pump applicable to its characteristic study, *J. CSME*, 11 (4) (1990) 385-391.
[5] S. C. Lee and S. N. Lee, Design and analysis of gerotor for hydraulic motors, *J. KSTLE*, 11 (2) (1995) 63-70.
[6] C. H. Kim, D. I. Kim, H. S. Ahn and T. H. Chong, Analysis of tooth contact stress of gerotor hydraulic motors, *J. KSTLE*, 15 (2) (1999) 164-170.
[7] J. H. Kim and C. Kim, Development of an integrated system of automated design of gerotor oil pump, *J. of KSPE*, 23 (2) (2006) 88-96.
[8] J. H. Kim, C. Kim and Y. J. Chang, Optimum design on lobe shapes of gerotor oil pump, *J. of Mechanical Science and Technology*, 20 (9) (2006) 1390-1398.
[9] Y. J. Chang, J. H. Kim, C. H. Jeon, C. Kim and S. Y. Jung, Development of an integrated system for the automated design of a gerotor oil pump, *J. of Mechanical Design*, 129 (2007) 1099-1105.

Sung-Yuen Jung is currently a Research Professor at the Research Institute of Mechanical Techno-logy at Pusan National University in Busan, Korea. He received his M.S. and Ph.D. degrees from Pusan National University in 2000 and 2005, respectively. His research interests include computer-aided process planning and die design, CAD/CAM and FEM simulation in metal forming process.

Seung-Moo Han received his B.S. degree in Mechanical Engineering from YeungNam University, Korea, in 1986. He then received his M.S. from Yonsei University, Korea in 1990 and Ph.D. degrees from the State University of New York at Buffalo, USA in 1996. Professor Han is currently a Professor at the Department of Biomedical Engineering School of Electronics and Information at Kyung Hee University in Gyeonggi-do, Korea. His research fields extend into biomedical engineering, medical imaging and biosignal processing.

Hae-Yong Cho received his B.S. degree in Mechanical Engineering from Pusan National University, Korea, in 1983. He then received his M.S. and Ph.D. degrees from Pusan National University in 1985 and 1991, respectively. Professor Cho is currently a Professor at Department of Mechanical Engineering and a Director of Development of the Electrical Power Apparatus Core Technology Center at the Chungbuk National University in Cheongju-si Chungbuk, Korea. His research fields extend into CAD/CAM and FEM simulation in metal forming process.

Chul Kim received his B.S. degree in Mechanical Engineering from Pusan National University, Korea, in 1985. He then received his M.S. and Ph.D. degrees from Pusan National University in 1987 and 1997, respectively. Professor Kim is currently a Professor at the Research Institute of Mechanical Technology at Pusan National University in Busan, Korea. His research fields extend into process planning, die design, CAD/CAM, and FEM simulation in metal forming process.